





# Development of Curcumin and Turmerone Loaded Solid Lipid Nanoparticle for Topical Delivery: Optimization, Characterization and Skin Irritation Evaluation with 3D Tissue Model

Beyza Sümeyye Aydın <sup>1,\*</sup>, Ali Asram Sagioglu <sup>2,3,\*</sup>, Dilek Ozturk Civelek <sup>4</sup>, Mustafa Gokce <sup>4</sup>, Fatemeh Bahadori<sup>5</sup>

<sup>1</sup>Bezmalem Vakif University, Health Sciences Institute, Department of Biotechnology, Istanbul, 34093, Turkey; <sup>2</sup>Istanbul University-Cerrahpasa, Faculty of Pharmacy, Department of Pharmaceutical Technology, Istanbul, 34500, Turkey; <sup>3</sup>Bezmalem Vakif University, Faculty of Pharmacy, Department of Pharmaceutical Technology, Istanbul, 34093, Turkey; <sup>4</sup>Bezmalem Vakif University, Faculty of Pharmacy, Department of Pharmacology, Istanbul, 34093, Türkiye; <sup>5</sup>Istanbul University-Cerrahpasa, Faculty of Pharmacy, Department of Analytical Chemistry, Istanbul, 34500, Turkey

\*These authors contributed equally to this work

Correspondence: Ali Asram Sagioglu, Istanbul University-Cerrahpasa, Faculty of Pharmacy, Department of Pharmaceutical Technology, Istanbul, Turkey, Email [a.a.sagioglu@gmail.com](mailto:a.a.sagioglu@gmail.com); Beyza Sümeyye Aydın, Bezmalem Vakif University, Health Sciences Institute, Department of Biotechnology, Istanbul, Turkey, Email [beyza\\_sumeyye@hotmail.com](mailto:beyza_sumeyye@hotmail.com)

**Background:** *Curcuma longa* L., commonly known as turmeric, is renowned for its therapeutic benefits attributed to bioactive compounds, namely curcumin (Cur) and aromatic turmerone (Tur), present in its rhizome. These compounds exhibit diverse therapeutic properties, including anti-inflammatory, antioxidant, and anti-tumor effects. However, the topical application of these compounds has a significant potential for inducing skin irritation. This study focuses on formulating solid lipid nanoparticle (SLN) carriers encapsulating both Cur and Tur for reduced irritation and enhanced stability.

**Methods:** SLN formulations were prepared by a method using homogenization followed by ultrasonication procedures and optimized by applying response surface methodology (RSM).

**Results:** The optimized SLN formulation demonstrated entrapment efficiencies, with  $77.21 \pm 4.28\%$  for Cur and  $75.12 \pm 2.51\%$  for Tur. A size distribution of  $292.11 \pm 9.43$  nm was obtained, which was confirmed to be a spherical and uniform shape via environmental scanning electron microscopy (ESEM) images. The in vitro release study indicated cumulative releases of  $71.32 \pm 3.73\%$  for Cur and  $67.23 \pm 1.64\%$  for Tur after 24 hours under sink conditions. Physical stability tests confirmed the stability of formulation, allowing storage at 4°C for a minimum of 60 days. Notably, in vitro skin irritation studies, utilizing the reconstructed human epidermal model (EPI-200-SIT), revealed a significant reduction in irritation with the SLN containing Cur and Tur compared to nonencapsulated Cur and Tur.

**Conclusion:** These findings collectively endorse the optimized SLN formulation as a favorable delivery system for Cur and Tur in diverse topical uses, offering enhanced stability, controlled release and reduced irritation.

**Keywords:** curcumin, aromatic turmerone, skin irritation, reconstructed human epidermal model, solid lipid nanoparticle, response surface methodology

## Introduction

The principal bioactive compounds isolated from *Curcuma longa* L. are curcuminoids, sesquiterpenoids, and turmerones.<sup>1</sup> Curcumin (Cur), derived from the dried rhizomes of *Curcuma longa* L., is a polyphenolic compound recognized for its diverse therapeutic effects. It is the primary therapeutic component of the turmeric plant and exhibits anti-oxidant, anti-inflammatory, antimicrobial, anticancer, antipsoriatic, and wound-healing activities.<sup>2,3</sup> Due to these therapeutic activities, Cur is used topically for skin aging, infections, acne, psoriasis, eczema, dermatitis-like inflammations, and skin cancer. Therefore, Cur

is bioactive with enormous potential for skin and skin diseases due to its therapeutic activity.<sup>4,5</sup> However, as with any therapeutic agent, the use of Cur in topical applications is not without its challenges, chief among them being the potential for skin irritation. Skin irritation, characterized by redness, itching, or discomfort, can pose a significant hurdle to the widespread adoption of Cur-based topicals. Various factors contribute to this concern, including poor solubility of Cur and the necessity for high concentrations to achieve therapeutic effects.<sup>2,6</sup>

Aromatic Turmerone (Tur), one of the key components found in turmeric and its essential oil, has garnered attention for its varied therapeutic properties, encompassing anti-oxidant, anti-tumor and anti-cancer activities.<sup>7-10</sup> The therapeutic potential of Tur extends to the realm of dermatology, particularly in the management of inflammatory skin conditions. Notably, topical applications of Tur have demonstrated efficacy in alleviating skin inflammation in murine models by modulating the expression of key cytokines, presenting itself as a promising candidate for treating inflammatory skin diseases such as psoriasis.<sup>11</sup> Cur and Tur exist together within the plant's rhizome. According to information obtained from previous studies, absorption of Cur is significantly enhanced in the presence of Tur, as compared to Cur alone, emphasizing the potential synergistic benefits of these compounds.<sup>12-15</sup> The synergistic effects of Cur and Tur have been investigated, revealing enhanced anti-inflammatory activity when compared to standard Cur alone.<sup>16,17</sup>

In the dynamic landscape of dermatological formulations, the advent of nanocarrier systems such as liposomes, polymeric nanoparticles, lipid-based carriers and nanoemulsions has introduced groundbreaking approaches to drug delivery methods, offering the potential of improved effectiveness and fewer side effects. Among these, solid lipid nanoparticles (SLNs) have proven to be a novel approach, especially for topical applications.<sup>18,19</sup> Unlike liposomes, SLNs have a solid lipid matrix, which provides enhanced stability and protection against degradation.<sup>20</sup> In contrast to polymeric nanoparticles, SLNs are composed of biodegradable lipids, reducing concerns about long-term toxicity.<sup>21,22</sup> Additionally, when compared to nanoemulsions, SLNs provide controlled drug release due to their solid nature.<sup>23,24</sup> When applied topically, SLN exhibits remarkable potential to penetrate the uppermost layer of the skin and reach its deeper layers, thereby optimizing drug delivery to target sites.<sup>25</sup> This enhanced penetration leads to improved bioavailability of both hydrophobic and hydrophilic drugs. In addition, the biocompatibility of the lipid components in SLN contributes to their safety profile for skin applications.<sup>26,27</sup> Topical applications encounter challenges, including skin irritation, difficulties in achieving optimal skin permeation, ensuring drug stability, bioavailability concerns, and maintaining dose uniformity.<sup>28,29</sup> Traditional formulations may cause skin irritation due to their composition, occlusive nature, or interactions with the skin barrier.<sup>30</sup> However, SLNs, with their biocompatible lipid matrix, offer a promising avenue to alleviate these concerns.<sup>31,32</sup>

Formulation optimization involves navigating a complex landscape of variables, where the interplay of factors can significantly impact the desired outcomes. Traditional approaches have been the cornerstone of formulation design, involving the systematic adjustment of one factor while keeping others constant.<sup>33,34</sup> However, these methods often fall short in capturing the intricate interactions among multiple variables, leading to suboptimal formulations and resource-intensive trial-and-error processes. In contrast, response surface methodology (RSM) emerges as a robust and systematic statistical technique designed to navigate the intricate design space efficiently. By modeling the relationships between multiple factors and responses, RSM allows researchers to explore the synergistic or antagonistic effects of variables, ultimately identifying the optimal formulation conditions. This not only accelerates the formulation optimization process but also minimizes the need for exhaustive experimental trials. Numerous studies in the literature have demonstrated the superior efficiency of RSM in achieving optimal formulations with fewer experimental runs compared to traditional approaches.<sup>35,36</sup>

This study aims to develop safe and efficient novel topical formulations loaded with Cur and Tur and evaluate the skin irritation levels of the formulations. SLN formulations were prepared using hot homogenization and ultrasonication procedures. Additionally, the optimization of formulations was studied using a central composite design (CCD). The SLN system was evaluated for its *in vitro* characterization and skin irritation properties.

## Materials and Methods

### Materials

Curcumin (Cur) was purchased from Sigma Aldrich. Aromatic Turmerone was supplied from Cayman Chemical. Compritol<sup>®</sup> ATO 888 was kindly donated from Gattefossé, France. Plantacare<sup>®</sup> 810 UP (caprylyl/capryl glucoside)

was a friendly donation from BASF, Turkey. Dialysis membrane (Spectra/por 4, d: 16 mm, Mw: 12–14 kDa) was obtained from Spectrum Chemical Mfg. Corp. (USA). The cell line was supplied from American Type Culture Collection (ATCC). Fetal calf serum, RPMI medium, PBS, and Dulbecco's Modified Eagle's Medium-F12 were all obtained from GIBCO BRL, InVitrogen (Carlsbad, CA). A three-dimensional, reconstructed human epidermal model (EPI-200-SIT) including human-derived epidermal keratinocytes was purchased from MatTek Corporation. The chemicals, solvents, and reagents employed in this research were all of analytical quality.

## Preparation of Cur-Tur-Loaded SLN

Cur-Tur loaded SLN formulations were prepared by a method using hot homogenization and ultrasonication procedures.<sup>37</sup> Cur (0.02% w/v) and Tur (0.1% w/v) were mixed with Compritol ATO 888 (C888) as a solid lipid. Then, the mixture was melted at 85 °C and blended with magnetic stirring at 300 rpm until Cur and Tur were completely dissolved. The water phase, Plantacare 810 (P810) solution, was preheated to 85 °C and slowly added to the lipid phase through Ultra-Turrax and homogenized for 5 min at 20,000 rpm (Ultra-Turrax T25, IKA-Werke GmbH & Co. KG, Staufen, Germany). An ultrasonic probe was used for 10 min. Subsequently, the formulations were given time to reach room temperature. The same approach was utilized to prepare blank SLN, without including Cur and Tur.

## Experimental Design

The RSM was employed to optimize the formulated SLN dispersion. Based on prior research and analysis, the combination of C888 and P810 was identified as two pivotal variables influencing the characteristics of the SLN.<sup>38,39</sup> The effects of these factors on the SLN were thoroughly analyzed using CCD, with five separate levels ( $-\alpha$ ,  $-1$ ,  $0$ ,  $1$ ,  $+\alpha$ ). A selected  $\alpha$  value of 1.44 was employed to maintain orthogonality and rotatability of the design. To enhance the accuracy of the methodology, 13 trials were conducted, including four factorial points, four axial points, and five repeated experiments (see Table 1 for details). Response variables were chosen as entrapment efficiency of Cur and particle size.

The experimental design and subsequent statistical analysis were conducted using the Design-Expert software (version 13.0.5.0). The evaluation of the experimental outcomes was performed employing a nonlinear quadratic equation represented as follows:

$$Y : \beta_0 + \beta_1 A + \beta_2 B + \beta_{12} AB + \beta_{11} A^2 + \beta_{22} B^2$$

In this equation,  $Y$  signifies the predicted response, while  $A$  and  $B$  represent the independent variables, the terms of  $A^2$  and  $B^2$  denote the interaction and quadratic components, respectively.  $\beta_0$  is the intercept value,  $\beta_1$  and  $\beta_2$  are linear coefficients,  $\beta_{12}$  signifies the interaction coefficient,  $\beta_{11}$  and  $\beta_{22}$  represent quadratic coefficients.

The impact of the independent factors on the outcomes was evaluated utilizing Analysis of Variance (ANOVA), with a significant value of  $p < 0.05$ . Appropriateness of this model was determined by examining the determined predicted and adjusted correlation coefficients ( $r^2$ ). Three-dimensional surface graphs were employed to visually represent how the chosen independent variables impact the quality of the SLN dispersion. The optimum SLN dispersion was identified based on responses that yielded the higher entrapment efficiency of Cur and the smaller particle size values. This optimum SLN dispersion was replicated three times, and the achieved outcomes were contrasted with the predicted levels.

**Table 1** Chosen Parameters in CCD

Variables		Level of Variables				
		-1.41	-1	0	1	1.41
A	C888 (%w/v)	0.47	0.8	1.6	2.4	2.73
B	P810 (%w/v)	0.23	0.4	0.8	1.2	1.37

**Abbreviations:** C888: Compritol® ATO 888; P810: Plantacare® 810; w/v: Weight/Volume.

## Determination of the Particle Size, Polydispersity, and Zeta Potential

Using the Zetasizer Nano ZSP (Malvern Instruments Ltd, Malvern, UK) at 25 °C and a 173° angle, particle size and PDI values of SLN were assessed. Through the use of specialized apparatus and the micro-electrophoresis method, zeta potential values were determined (Malvern Instruments Ltd).<sup>40</sup> In order to avoid scattering effects, SLN formulations were diluted (1:100) with ultrapure water. At least three times each formulation was measured.

## Determination of the Entrapment Efficiency

The measurement of the entrapment efficiency of SLN was performed using the centrifugation procedure, as described in previous studies.<sup>41,42</sup> The Cur-Tur-loaded SLN formulation (1.5 mL) underwent centrifugation at 15,000 rpm for one hour to the un-entrapment drug from the drug that had been entrapped. After centrifugation, the formulation was dissociated into two phases: pellet and liquid supernatant. Each phase was transferred into the new Eppendorf. The pellets were made up to 2 mL with ACN and vortexed. By diluting with ACN (1:100) supernatant and pellet samples were prepared. Finally, measurements were taken with the Reverse Phase High-Performance Liquid Chromatography method (RP-HPLC). The determination of entrapment efficiency was conducted according to the formulation below:

$$\text{Entrapment Efficiency}\% = \frac{W_a - W_b}{W_b} * 100$$

Where  $W_a$  is the initial quantity of the drugs introduced to the SLN dispersion and  $W_b$  is the quantity of un-entrapment drugs in the supernatant.

## Total Drug Content of SLN

To assess the Cur and Tur content in the optimum SLN formulation, 200  $\mu$ L samples of the SLN suspension were solubilized in acetonitrile. The solution obtained was subsequently passed through a membrane filter with a pore size of 0.45  $\mu$ m, and the concentrations of Cur and Tur were assessed using a validated RP-HPLC technique.<sup>43</sup>

## Analytical Method for Cur and Tur Determination

A Shimadzu LC20-AT HPLC system (Shimadzu, Kyoto, Japan) along with a Shimadzu SPD-20A UV-Vis detector was employed to quantify Cur and Tur.<sup>44</sup> As a mobile phase, acetonitrile:phosphate buffer (adjusted to pH 3.0 using phosphoric acid) (80:20, v/v) for Cur and acetonitrile:ultrapure water containing 0.4% (v/v) acetic acid (45:55, v/v) for Tur were applied after filtration and degasification. Through a C18 column (250  $\times$  4.6 mm; 5  $\mu$ m – GL Sciences Inert Sustain) preserved at 35 °C, the separation took place with a low-pressure gradient, a flow rate of 1.0 mL/min of the mobile phase. The injection level was 20  $\mu$ L, and the UV detector was configured at 420 nm for Cur detection and 240 nm for Tur detection.

The validation investigations were conducted in a manner that was consistent with the guidelines outlined in the ICH-Q2 protocols. In the assessment of linearity, standard curves were generated using the stock solution of Cur and Tur over the concentration range of 0.05 to 20  $\mu$ g/mL. The analysis revealed a direct correlation among the peak areas and the concentrations of Cur ( $r^2=0.9994$ ) and Tur ( $r^2=0.9991$ ) within the 0.05–20  $\mu$ g/mL range. Additionally, assessments conducted with blank SLN demonstrated no discernible interference with the peaks of Cur and Tur, affirming the selectivity of method. Moreover, the validation of the RP-HPLC method encompassed examinations of accuracy, precision, and stability.

## Morphological Characterization

The morphological examination of the optimum formulation was conducted using environmental scanning electron microscopy (ESEM) instrument, specifically the Thermo Fisher Quattro ESEM.<sup>45</sup> The dispersion of SLN was diluted with deionized water prior to analysis. A drop of SLN was carefully put onto a copper grid coated with carbon and allowed to evaporate at room temperature, resulting in the formation of a ultra-thin layer. After drying, the formulation was imaged at 30 kV and in STEM mode.

## In vitro Release Study

The dialysis method was employed to investigate the in vitro release of drugs from the optimized SLN formulations.<sup>46,47</sup> Dialysis membranes (cellulose membrane, 12.000–14.000 Dalton MWCO) were immersed in double-distilled water for 30 minutes before the experiment. Three parallel SLN formulations (2 mL) were added to the dialysis bags sealed using standard closures. These bags were then placed in a solution comprising 75 mL of PBS: Tween 80 (19:1; pH 7.4) and sealed with parafilm and aluminum to prevent the evaporation of the receptor phase. The procedure was conducted in a shaking incubator at a constant temperature of  $32\text{ }^{\circ}\text{C} \pm 0.5\text{ }^{\circ}\text{C}$  and a rotating rate of 100 rpm/min. At designated intervals (0, 0.25, 0.5, 1, 2, 3, 4, 5, 6, 8, and 24 h), 0.5 mL aliquots were obtained from the receiving phase and replaced with an equal volume of fresh medium to sustain sink conditions. The quantification of released Cur and Tur was carried out using a validated RP-HPLC method.

## Stability of SLN

To evaluate the stability studies, optimized Cur-Tur-loaded SLN was observed and measured for a duration of two months, during storage at a temperature of  $5^{\circ}\text{C} \pm 3^{\circ}\text{C}$ .<sup>48</sup> The formulations were analyzed at defined time intervals for various parameters, including physical appearance, particle size, PDI value, and zeta potential. The experiments were performed three times.

## In vitro Skin Irritation Studies

The study was conducted by a validated and utilized epidermis equivalent kit, EpiDerm™, for the in vitro skin irritation test.<sup>49,50</sup> The parameters that were assessed in this study included the percentage of cell viability as determined by the MTT reduction assay.

## Conditioning of EpiDerm Tissues

The assay medium (EPI-100-NMM) was let to reach room temperature ( $20\text{--}25\text{ }^{\circ}\text{C}$ ). The tissue inserts were put onto the 6-well plates containing the 0.9 mL assay media after the Epiderm package was taken out of the refrigerator. The EpiDerm tissues were placed in 6-well plates and transferred to a  $37\text{ }^{\circ}\text{C}$  incubator with 5%  $\text{CO}_2$  for  $18 \pm 3$  hours.<sup>51</sup>

## Dosing and Exposure

After  $18 \pm 3$  hours of incubation, the assay mediums in the six-well plates were replaced with 0.9 mL of new, assay medium in each well. A 5% SDS solution supplied with EPI-200-SIT kit was used as positive controls and inserts treated with sterile DPBS were used as the negative control. Then, 30  $\mu\text{L}$ /insert of the tested samples were applied to the tissues. The dosed EpiDerm tissues were placed in 6-well plates, which were then placed back in the incubator for 24 hours. Afterward, inserts were rinsed with sterile DPBS in case of any test substances remained on the tissues after exposure. This process was repeated for each insert, separately and carefully. Lastly, inserts were fully submerged into DPBS to completely remove any residue.

## MTT Viability Assay

After a 24-hour incubation, MTT medium was prepared freshly and pipetted 300  $\mu\text{L}$  of MTT medium in each well of a new 24-well plate. Then, inserts were blotted from the bottom and transferred to a plate prefilled with MTT medium. Following the 3-hour MTT incubation, each insert was taken out, blotted with a sterile gauge from the bottom, and then placed onto the 24-well extraction plate. The blue formazan was dissolved by adding 2 mL of isopropanol as an extractant per tissue. The cell culture inserts were submerged into an extractant solution to completely cover the EpiDerm tissues. The plate was put within a sealable bag and run at room temperature for 2 hours at 120 rpm. The extraction fluid was pipetted to ensure mixing after the extraction phase ended. For the final step, 200  $\mu\text{L}$  of each tissue extract was put into a 96-well microtiter plate to detect formazan crystal's optical density using a spectrophotometer at 570 nm.<sup>52</sup>

## Statistical Analyses

The experiments were conducted in triplicate at minimum, and the data are expressed as the mean  $\pm$  standard deviation (SD). Statistical analysis involved one-way ANOVA with Tukey's post hoc test. Statistical significance was considered at a level of  $p < 0.05$ . Following the exclusion of blank optical density (OD) values from the initial absorbance data for skin irritation test, the mean OD and standard deviation were calculated for each test. The mean OD of the untreated tissues used as the negative control was accepted as 100% viability. The outcomes were articulated as a percentage of viability relative to the negative control, with the accompanying SD, for each insert.

## Results and Discussion

### Experimental Design of SLN

#### Impact of Independent Variables on Entrapment Efficiency

The outcomes of the entire set of 13 experiments are presented in Table 2, in conjunction with the CCD matrix. The SLN dispersions demonstrated an entrapment efficiency of Cur that varied within the range of 48.39% to 90.97%. The determination of entrapment efficiency responses was established utilizing the associated quadratic equation.

$$R1 : 67.53 + 11.83A + 8.71B - 7.97AB + 2.32A^2 - 3.02B^2$$

In evaluating the predictive performance of the regression model for entrapment efficiency (R1), it is important to consider the encoded parameters (A and B) for C888 and P810, respectively. The results of the analysis, as presented in Table 3, reveal compelling evidence of the model's statistical significance. This is evident from the substantial F value of 72.79 and the remarkably low P-value of under 0.0001, indicating that the model is highly reliable for predicting entrapment efficiency of Cur. Furthermore, the lack of fit value, with a p-value of 0.417, provides additional support for the model's appropriateness in fitting the data adequately. The high coefficient of determination ( $R^2$ ) value of 0.9811 is particularly noteworthy, implying that approximately 98.1% of the variability in the response variable (entrapment efficiency of Cur) can be explained by this regression model. In addition, the adjusted and predicted  $R^2$  values of 0.9677 and 0.9209, respectively, further underscore the model's robustness. These values, both exceeding 0.9, indicate a high degree of correlation between the observed and predicted data. This level of concordance is substantial, given that the variation in these metrics is less than 0.2. The results of the ANOVA analysis and the associated regression metrics collectively demonstrate the efficacy of the model in accurately predicting the entrapment efficiency of Cur.

**Table 2** CCD Matrix and Obtained Responses for SLN

Run	Variables		Responses	
	A: C888	B: P810	Particle Size (nm)	Entrapment Efficiency (%)
1	0.8	1.2	230.9	72.43
2	1.6	0.8	320.3	64.98
3	0.47	0.8	207.8	53.48
4	1.6	0.8	345.6	69.26
5	1.6	0.8	353.8	68.93
6	0.8	0.4	205.1	40.26
7	2.4	1.2	224.4	77.30
8	2.4	0.4	211.3	77.03
9	1.6	1.37	227.4	74.72
10	1.6	0.8	338.7	69.42
11	1.6	0.23	229.4	48.39
12	1.6	0.8	327.4	65.04
13	2.73	0.8	203.8	90.97



**Table 3** ANOVA Results for Entrapment Efficiency of Cur

Source	Sum of Squares	df	Mean Square	F Value	P-value Prob > F	
Model	2096.66	5	419.33	72.79	< 0.0001	significant
A-C888	1120.04	1	1120.04	194.43	< 0.0001	
B-P810	606.85	1	606.85	105.34	< 0.0001	
AB	254.40	1	254.40	44.16	0.0003	
A <sup>2</sup>	37.31	1	37.31	6.48	0.0384	
B <sup>2</sup>	63.41	1	63.41	11.01	0.0128	
Residual	40.32	7	5.76			
Lack of Fit	19.10	3	6.37	1.20	0.4168	not significant
Pure Error	21.23	4	5.31			
Cor Total	2136.98	12				

**Abbreviation:** df, degree of freedom.

The results obtained from the ANOVA analysis [Table 3](#), indicate that adjustments in the quantities of solid lipid and surfactant in the SLN formulation had a noticeable effect on entrapment efficiency ( $p < 0.05$ ). To further elucidate the impact of these independent variables on the outcome, three-dimensional response surfaces were employed, which is a widely accepted approach for a more comprehensive assessment of their effects. As depicted in [Figure 1A](#), the three-dimensional response surface graph illustrates that raising the level of solid lipid resulted in a notable enhancement in entrapment efficiency. This phenomenon can be explained by the increased solid lipid content providing more opportunities for lipophilic drug molecules to interact with the lipid matrix. Consequently, this creates a more favorable environment for the encapsulation and retention of lipophilic drugs within the lipid nanoparticles. Additionally, the observed increase in viscosity of the carrier system with higher amounts of solid lipid is likely to play a role in this enhancement. This increased viscosity leads to accelerated solidification of the particles, consequently restricting the diffusion of the drugs into the receptor phase.<sup>53,54</sup> In another study by Devin et al, noscapine-loaded SLNs were prepared, and it was determined that the entrapment efficiency of the lipophilic drug increased with the increase in the amount of solid lipid.<sup>55</sup> Furthermore, our study demonstrates that an increased quantity of surfactant also positively impacts entrapment efficiency. This is due to the fact that increased surfactant concentrations contribute to improved stability of the SLN by reducing interfacial tension and preventing aggregation. Stable nanoparticles, in turn, exhibit greater efficacy in retaining hydrophobic drug. Surfactants perform a crucial function in the emulsification process during SLN

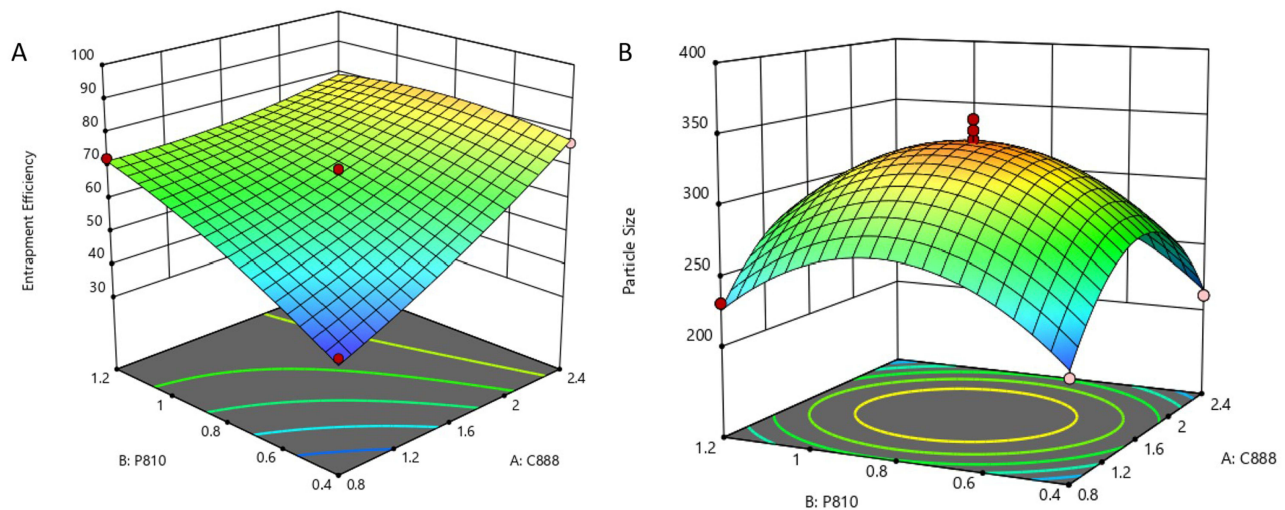


**Figure 1** Three-dimensional response surface graphs of SLN (A) for entrapment efficiency of Cur and (B) for particle size values.

preparation. Proper emulsification results in smaller, more uniform nanoparticles with a higher surface area, providing more opportunities for effective drug encapsulation.<sup>56,57</sup> The findings from this study underscore the significance of optimizing the solid lipid and surfactant quantities in SLN formulations to enhance entrapment efficiency.

### Impact of Independent Variables on Particle Size

The particle size analysis of the SLN dispersions revealed a range of sizes, varying from 203.8 to 353.8 nm, as outlined in Table 2. To model these outcomes, a quadratic equation was employed, represented as:

$$R^2 : 337.16 - 0.732A + 4.52B - 3.2AB - 65.48A^2 - 54.18B^2$$

In the current study, particle size ( $R^2$ ) was investigated as a function of encoded parameters A and B, corresponding to C888 and P810, respectively. The regression model's performance was assessed using the ANOVA table provided in Table 4. The obtained results indicate a high degree of statistical significance for the model. This is evident from the notably high F value of 65.73 and an associated p-value of less than 0.0001. The  $R^2$  value of 0.9791 further supports the model's effectiveness in explaining the variability in particle size. This value suggests that approximately 97.91% of the observed variability can be accounted for by the proposed model. Additionally, the proximity of the adjusted  $R^2$  (0.964) and predictive  $R^2$  (0.94) values, with a difference of less than 0.2, underscores the model's compatibility in describing the relationship between the encoded parameters and particle size. These findings collectively validate the capability of the regression model for predicting particle size based on the encoded parameters A and B.

The ANOVA results presented in Table 4 provided information on the impact of varying the amounts of formulation components on the size of the SLN. Specifically, variations in the amount of P810 exhibited a statistical significant effect ( $p < 0.05$ ), whereas changes in the quantity of C888 did not demonstrate statistical significance ( $p > 0.05$ ) on the size. This indicates that the amount of P810 played a more substantial role in determining the particle size compared to C888. The effect of surfactant levels on SLN size was further elucidated through a three-dimensional response surface graph, shown in Figure 1B. It was observed that as the amount of surfactant increased within a certain range, the particle size increased correspondingly. Specifically, as the surfactant quantity was raised from 0.4% to 0.8%, a concurrent increase in particle size was detected. However, beyond that range, higher surfactant values appeared to lead to a reduction in particle size. Several factors could be responsible for this intriguing phenomenon, including a potential surfactant saturation point or changes in the microenvironment of the SLN formation process. The excess surfactant could alter the physicochemical properties of the lipid matrix or promote the formation of smaller nanoparticles through enhanced steric stabilization.<sup>58</sup> The experimental data and graphical representation suggest a nuanced relationship between surfactant concentration and particle size in the context of SLN formulation. The observed increase in particle size to a given threshold, and subsequent decrease, underscores the importance of precise surfactant control in achieving the desired particle characteristics.

**Table 4** ANOVA Results for Particle Size

Source	Sum of Squares	df	Mean Square	F Value	P-value Prob > F	
Model	44,776.53	5	8955.31	65.73	< 0.0001	Significant
A-C 888	4.29	1	4.29	0.0315	0.0642	
B-P810	163.55	1	163.55	1.20	0.0095	
AB	40.96	1	40.96	0.3006	0.0005	
A <sup>2</sup>	29,826.99	1	29,826.99	218.92	< 0.0001	
B <sup>2</sup>	20,420.68	1	20,420.68	149.88	< 0.0001	
Residual	953.72	7	136.25			not significant
Lack of Fit	223.70	3	74.57	0.4086	0.7560	
Pure Error	730.01	4	182.50			
Cor Total	45,730.24	12				

**Abbreviation:** df, degree of freedom.



## Optimization Study of SLN

The process of identifying the optimized SLN formulation was carried out through the utilization of Design-Expert software, leveraging the dataset derived from the CCD matrix. The establishment of targeted limits was based on the consideration of achieving maximum entrapment efficiency of Cur and minimizing particle size values of SLN. Through statistical computations, the critical parameters for the formulation, denoted as C888 and P810, were determined to be 2.22% and 0.83%, respectively. The chosen parameters were then used to prepare the optimized SLN formulation in three times, aiming to validate the predictive precision of the model under ideal conditions. When the experimental findings were contrasted with the predicted outcomes, as detailed in Table 5, it was evident that the experimental data closely matched the model's predictions. This alignment between the predicted and observed results underscores the reliability and significance of the model. It indicates that the strategy used for the optimization of formulation effectively facilitated the identification of the optimal SLN formulation, ensuring that it met the desired criteria for entrapment efficiency of Cur and particle size.

The centrifuge method was employed to analyze the entrapment efficiency of Tur in the optimum SLN formulation. Entrapment efficiency of Tur in the optimum SLN formulation was a remarkable  $75.12 \pm 2.51\%$ , demonstrating the success of this lipophilic compound in the SLN matrix. The physicochemical properties of Tur play a crucial role in determining its entrapment efficiency. Tur, being a lipophilic compound, is expected to have a higher affinity for the lipid matrix of SLN, which can positively influence its entrapment efficiency.

The zeta potential, a parameter indicative of the surface charge of colloidal dispersions, serves as a crucial descriptor for understanding the behavior of molecules and nanoparticles within these systems. Its significance lies in its ability to assess the stability of colloidal dispersions and provide insights into the interactions between colloidal particles. In this study, optimum SLN formulation exhibited a zeta potential of  $-37.8 \pm 1.4$  mV, indicating a negatively charged surface. Considering the nature of the stabilizer used, namely P810, a polyhydroxy surfactant with nonionic properties, one might anticipate a lower zeta potential. This expectation stems from the inherent steric stabilization provided by nonionic surfactants. However, our measurements reveal a relatively higher zeta potential, suggesting the presence of additional charges originating from adsorbed ion or surfactant on the surface. The structure of P810 further sheds light on this observation. It consists of a hydrophobic anchor incorporated into the surface, coupled with an extended hydrophilic tail made up of glucose molecules extending into the aqueous phase. This configuration facilitates strong interactions with water molecules, potentially attracting negatively charged hydroxyl ions. These interactions likely contribute to the observed zeta potential, indicating a complex interplay of surface charges and molecular structure.<sup>58,59</sup>

In evaluating the particle size distribution within our formulations, dynamic light scattering was employed to calculate the polydispersity index (PDI). This metric is crucial in providing insights into the homogeneity of particle sizes, ultimately influencing the stability and performance of the formulation over time. To maintain the stability of a nanoparticle formulation, it is imperative that the polydispersity index remains within an acceptable range. High values indicate a broad range of particle sizes and a greater variability, which can lead to issues such as aggregation or sedimentation over time. In contrast, low polydispersity indices signify a more uniform and narrow size distribution, which is desirable for achieving formulation stability and ensuring consistent performance. In this study, optimum SLN formulations typically exhibit a polydispersity index below a threshold value of 0.3. This signifies that the size distribution of SLN is appropriately narrow, with limited variability among the particles. Such a well-controlled size distribution is essential for the uniform dispersion of SLN within the formulation and their ability to resist aggregation or precipitation.

**Table 5** Predicted and Experimental Responses of the Optimized SLN

Responses	Predicted Value	Experimental Value	Prediction Error (%)
Entrapment Efficiency (%)	78.21	77.21±4.28	1.01
Particle Size (nm)	297.37	292.11±9.43	1.77

## Drug Content of SLN Formulation

In this study, an essential aspect was to assess the content of Cur and Tur within the SLN dispersions. This evaluation served to gauge any potential loss of drugs that might have transpired during the formulation process of the optimized SLN dispersions. Our experiments revealed a notably high recovery rate for both Cur and Tur, with approximately  $97.21\% \pm 0.72\%$  of Cur and  $95.45\% \pm 1.21\%$  of Tur retrieved from the SLN dispersions. This robust recovery indicates the efficiency of the preparation method, highlighting its suitability for these bioactive compounds. Such high levels of drug content indicate that the SLN dispersion process does not induce significant degradation or loss of the Cur and Tur. The drug content percentages obtained are consistent with data in the literature showing that high drug content percentages are obtained when SLN is used as a carrier system.<sup>60,61</sup>

## Morphology Studies

Verification of particle size values and the detailed examination of formulation morphology are integral aspects of assessing the characteristics of SLN. In alignment with best practices, particle size investigations were performed using both Zeta Sizer and electron microscopy techniques. It is noteworthy that the results obtained from these two methodologies exhibited a consistent correlation, reinforcing the reliability and accuracy of the particle size values reported. Moreover, The ESEM images, as depicted in Figure 2, elucidated a distinctive morphology characterized by a spherical and smooth surface. The correlation between particle size data from both Zeta Sizer and electron microscopy not only validates the precision of the measurement techniques but also provides a comprehensive understanding of the SLN physical characteristics.

## In vitro Release Study

The drug-release behavior of the optimized SLN was meticulously evaluated through the dialysis membrane diffusion method, a well-established technique for assessing the release of Cur and Tur. The selection of an appropriate membrane with a pore size calibrated to allow passage of the Cur and Tur while retaining the SLN proved crucial in ensuring accurate and reliable results. The in vitro release profiles, depicted in Figure 3, unveiled a distinct biphasic pattern across all formulations. This characteristic release profile encompasses an initial burst release phase succeeded by a more gradual and sustained release. In the case of our SLN formulations, the initial burst release accounted for  $48.21\% \pm 2.32\%$  for Cur and  $54.24\% \pm 4.51\%$  for Tur within the first 120 minutes. This phenomenon is often attributed to the rapid release of surface-associated molecules. Subsequently, a second, slower release phase ensued. This phase is believed to arise from the continuous diffusion of the Cur and Tur from within the bilayer structure of the SLN. This mechanism is particularly relevant for hydrophobic molecules, which may be situated within the lipid bilayer or on the exterior surface of the carrier system.

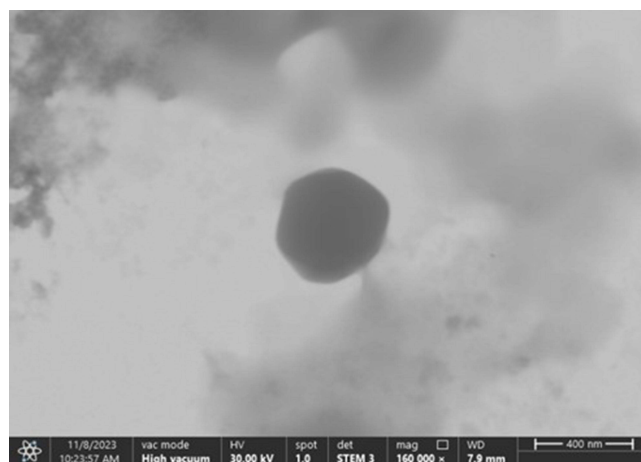


**Figure 2** ESEM images of optimized SLN.

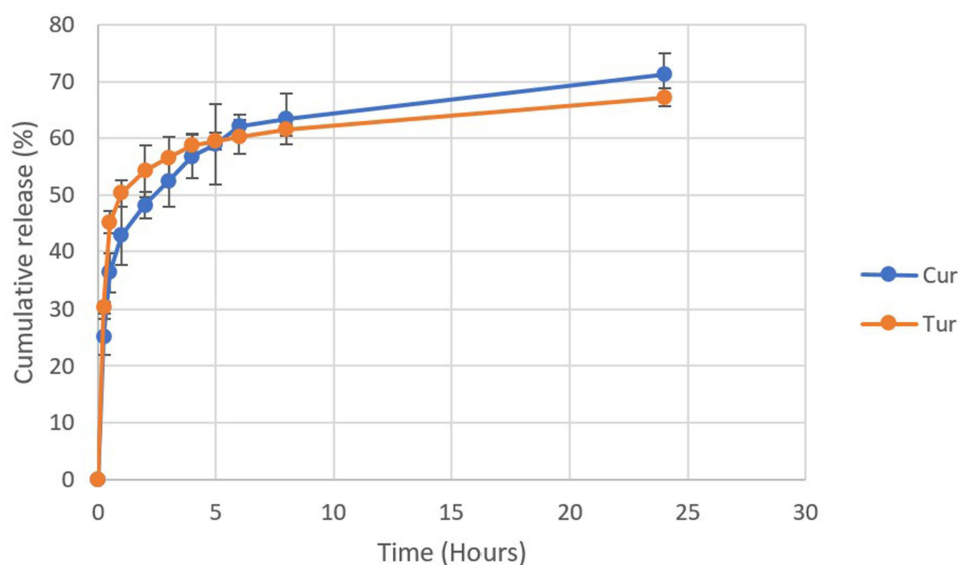


**Figure 3** Cur and Tur release profile from optimum SLN formulation.

Over a 24-hour period, an accumulated release of  $71.32\% \pm 3.73\%$  for Cur and  $67.23\% \pm 1.64\%$  for Tur was attained. These findings indicate a controlled and sustained release profile, which is highly advantageous for topical applications. This prolonged release not only ensures a consistent supply of drugs to the target area but also minimizes the need for frequent reapplication, thereby enhancing patient compliance. The initial burst release followed by a sustained phase exemplifies the potential of SLN in providing both immediate therapeutic effects and prolonged benefits over an extended period.

## Stability Studies

The stability analysis of the optimized SLN formulations was a crucial aspect of this study, involving a meticulous examination conducted over a period of 60 days in a controlled refrigerated environment at  $5 \pm 3^\circ\text{C}$ . This extended period enabled a thorough examination of the stability of formulations under storage conditions. The key parameters considered for monitoring included particle size, zeta potential, polydispersity index (PDI), and physical characteristics. The evaluation of zeta potential in SLN serves as an important determinant of colloidal stability. The zeta potential, which reflects the surface charge of nanoparticles, is crucial in predicting and preventing particle aggregation. The literature emphasizes that charged particles exhibiting a high zeta potential, typically exceeding  $\pm 30$  mV, are less prone to aggregation due to the strong electrostatic repulsion between them.<sup>62</sup> This repulsion counteracts the attractive van der Waals forces that tend to bring particles closer together. The measured zeta potential provides insight into the effectiveness of stabilizing agents used in SLN formulations and contributes to the formation of a charged layer around the nanoparticles.<sup>63</sup> The zeta potential of the optimum SLN formulation was measured to be  $-37.8 \pm 1.4$  mV, and a zeta potential value exceeding  $-30$  mV over the 60-day stability period is a positive indicator for the stability of SLN. The consistent maintenance of a high negative zeta potential over a long period of time means that electrostatic forces effectively counteract potential attractive forces that could lead to particle aggregation. This result is in agreement with the results in the literature that SLN with high negative zeta potential contributes positively to the stability of formulations.<sup>64,65</sup> Upon examining the results obtained at various intervals, as depicted in Figure 4, it is noteworthy that the particle size, zeta potential, and PDI of the optimized SLN exhibited no statistically significant variations throughout the 60-day storage period at  $5 \pm 3^\circ\text{C}$  ( $p > 0.05$ ). This consistent profile suggests the ability of formulations to maintain their structural and colloidal stability under specified storage conditions.

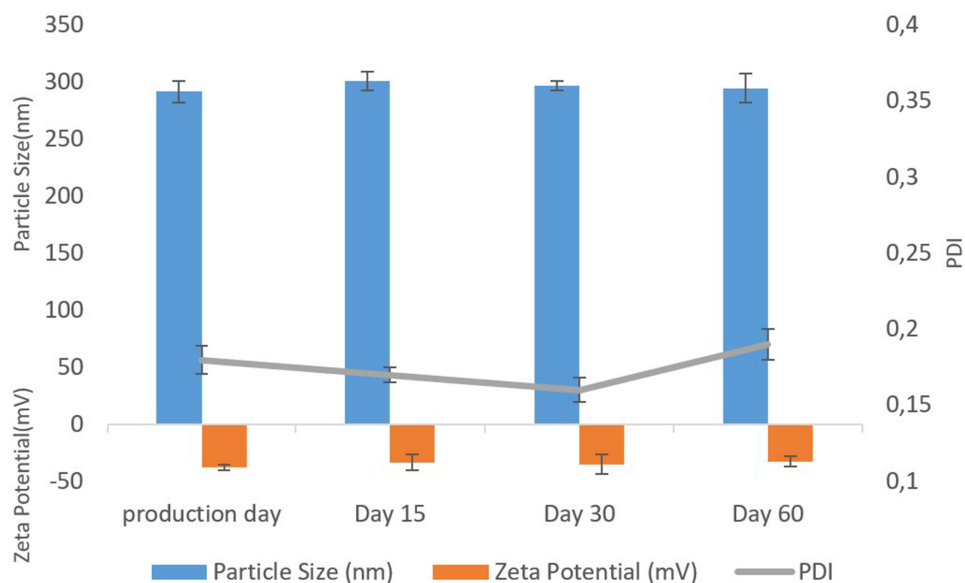


**Figure 4** The result of stability studies of optimum SLN.

## In vitro Skin Irritation Test

It is essential to evaluate the potential irritation of formulations in order to determine their ability to compromise cellular integrity and initiate local inflammatory processes. Skin damage may arise through two primary mechanisms: direct effects stemming from the physicochemical characteristics of the substance, such as lipid layer stabilization, pore formation, and destruction of skin tissues, and indirect effects involving the release of reactive oxygen species that disrupt dermal cell membranes.<sup>66,67</sup> In the pursuit of establishing reliable protocols for predicting the irritancy of various substances, the scientific community has long relied on the Draize skin irritation test, a methodology involving animal subjects that has been employed for over eight decades. However, the limitations of this approach, such as the observed differences in response among rabbits and humans, have prompted the search for more ethical and accurate alternatives.<sup>68</sup> Instead of focusing on the Draize test, *in vitro* models, particularly the reconstructed human epidermal model, have become increasingly important. These *in vitro* experiments adhere to established test guidelines, providing a more humane and scientifically robust means of classifying irritation and corrosive chemicals. The reconstituted human epidermis accurately replicates the biological characteristics of the typical human epidermis. It comprises non-transformed human-derived keratinocytes with representative histology and cytoarchitecture. *In vitro* skin irritation assays assess cellular responses to skin irritation, including cellular death and inflammation. These specific biomarkers are utilized to measure the potency of formulations to trigger skin irritation.<sup>69,70</sup> In the context of dermal drug carriers, especially when exploring potential applications of bioactive compounds like Cur and Tur, understanding and mitigating skin irritation risk is paramount. While these compounds exhibit remarkable biological activities, it is imperative to acknowledge that, like any active molecule, they may pose the risk of local irritation upon application. The findings of the present study as depicted in [Figure 5](#) reveal a statistically significant decrease in cell viability and irritant activity for the Cur and Tur mixture compared to both the NC group and the blank SLN formulation. However, when the Cur and Tur were encapsulated into the SLN formulation, there was no evidence of irritant effects of SLN, as the viability of each treated tissue remained above 90%. These results signify a pivotal finding in affirming the role of SLN as an effective carrier system in reducing the risk of irritation in topical applications. Another study by Harde et al developed an adapalene-containing SLN formulation and examined its skin irritation potential. According to the results of the skin irritation study conducted with the reconstructed human epidermis, the use of SLN as a carrier system significantly reduced the skin irritation potential of drug.<sup>71</sup> In essence, the utilization of SLN as a delivery system appears to mitigate the irritant potential of the bioactive compounds. This not only underscores the importance of carrier systems in modulating the biological effects of bioactive compounds but also has significant implications for the designing of

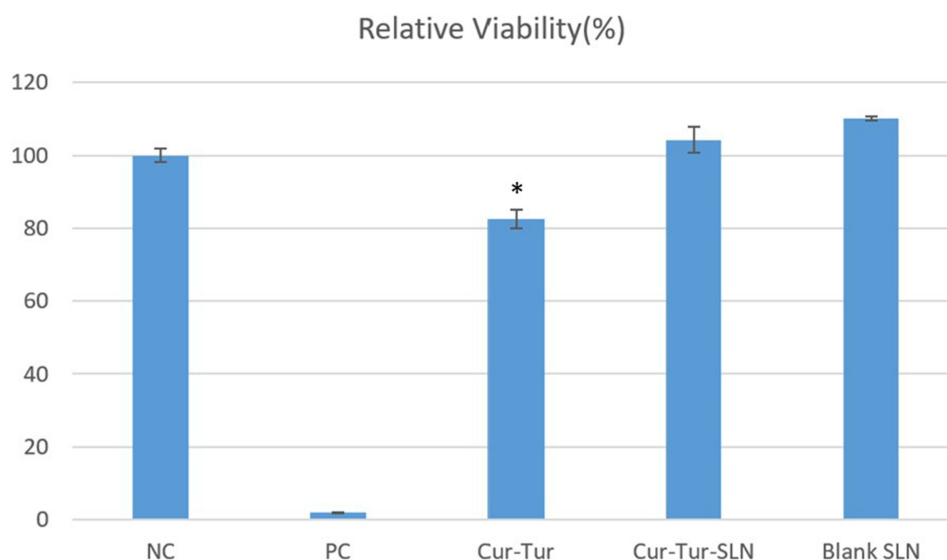


**Figure 5** In vitro irritation test with EpiDerm™. NC: negative control; DPBS, PC: positive control; 5% SDS, (\* $p < 0.05$ ).

dermal drug delivery systems aimed at optimizing therapeutic efficacy while minimizing potential adverse effects. These insights contribute to the ongoing discourse on refining in vitro testing methodologies and advancing the safety profiles of topical formulations.

## Conclusion

In this research, SLNs containing Cur and Tur, which represent a novel and promising approach for topical application, were successfully prepared and optimized to achieve high entrapment efficiency using RSM. The particle size, PDI and zeta potential values of the optimum SLN were satisfactory for topical delivery of bioactive components. In addition, ESEM imaging confirmed that the optimized SLN has a spherical structure and uniform size distribution. In vitro release profiles demonstrated controlled release of Cur and Tur from the SLN formulation. Stability assessments revealed that the optimized SLN maintained their stability over a 60-day period when stored under controlled conditions, a crucial factor for their practical applicability. In vitro skin irritation study utilizing the EPI-200-SIT model showed a significant reduction in irritation with the Cur-Tur-loaded SLN compared to the nonencapsulated Cur-Tur. This study positions SLN as a highly promising delivery system for the topical application of Cur and Tur. However, additional preclinical and clinical studies on irritation are needed to validate the efficacy of Cur-Tur-loaded SLN for minimizing skin irritation.

## Acknowledgments

This study was supported by Health Institutes of Türkiye (TUSEB) and Bezmialem Vakif University Research Fund (Projects No: 20210603).

## Disclosure

The authors report no conflicts of interest in this work.

## References

1. Nair A, Chattopadhyay D, Saha B. Plant-derived immunomodulators. *New Look to Phytomedicine Adv Herb Prod as Nov Drug Leads*. 2019;435–499. doi:10.1016/b978-0-12-814619-4.00018-5
2. Fuloria S, Mehta J, Chandel A, et al. A comprehensive review on the therapeutic potential of *Curcuma longa* Linn. in relation to its major active constituent curcumin. *Front Pharmacol*. 2022;13. doi:10.3389/fphar.2022.820806.
3. Vaughn AR, Branum A, Sivamani RK. Effects of turmeric (*curcuma longa*) on skin health: a systematic review of the clinical evidence. *Phytother Res*. 2016;30(8):1243–1264. doi:10.1002/ptr.5640



4. Somparn P, Phisalaphong C, Nakornchai S, Unchern S, Morales NP. Comparative antioxidant activities of curcumin and its demethoxy and hydrogenated derivatives. *Biol Pharm Bull.* 2007;30(1):74–78. doi:10.1248/bpb.30.74
5. Kundu JK, Na HK, Surh YJ. Ginger-derived phenolic substances with cancer preventive and therapeutic potential. *Forum Nutr.* 2009;61:182–192. doi:10.1159/000212750
6. Vareed SK, Kakarala M, Ruffin MT, et al. Pharmacokinetics of curcumin conjugate metabolites in healthy human subjects. *Cancer Epidemiol Biomarkers Prev.* 2008;17(6):1411. doi:10.1158/1055-9965.epi-07-2693
7. Chen Z, Quan L, Zhou H, et al. Screening of active fractions from curcuma longa radix isolated by HPLC and GC-MS for promotion of blood circulation and relief of pain. *J Ethnopharmacol.* 2019;234:68–75. doi:10.1016/j.jep.2018.09.035
8. Mansi K, Kumar R, Jindal N, Singh K. Biocompatible nanocarriers an emerging platform for augmenting the antiviral attributes of bioactive polyphenols: a review. *J Drug Deliv Sci Technol.* 2023;81:104269. doi:10.1016/j.jddst.2023.104269
9. Yang S, Liu J, Jiao J, Jiao L. Ar-Turmerone exerts anti-proliferative and anti-inflammatory activities in hacat keratinocytes by inactivating hedgehog pathway. *Inflammation.* 2020;43(2):478–486. doi:10.1007/S10753-019-01131-w
10. Sharma M, Grewal K, Jandrotia R, Batish DR, Singh HP, Kohli RK. Essential oils as anticancer agents: potential role in malignancies, drug delivery mechanisms, and immune system enhancement. *Biomed Pharmacother.* 2022;146:112514. doi:10.1016/j.biopha.2021.112514
11. Li YL, Du ZY, Li PH, et al. Aromatic-turmerone ameliorates imiquimod-induced psoriasis-like inflammation of BALB/c mice. *Int Immunopharmacol.* 2018;64:319–325. doi:10.1016/j.intimp.2018.09.015
12. Degot P, Huber V, Touraud D, Kunz W. Curcumin extracts from curcuma longa – improvement of concentration, purity, and stability in food-approved and water-soluble surfactant-free microemulsions. *Food Chem.* 2021;339:128140. doi:10.1016/j.foodchem.2020.128140
13. Meng FC, Zhou YQ, Ren D, et al. Turmeric: a review of its chemical composition, quality control, bioactivity, and pharmaceutical application. *Nat Artif Flavor Agents Food Dye.* 2018:299–350. doi:10.1016/b978-0-12-811518-3.00010-7
14. Patel S, Gogna P. Tapping botanicals for essential oils: progress and hurdles in cancer mitigation. *Ind Crops Prod.* 2015;76:1148–1163. doi:10.1016/j.indcrop.2015.08.024
15. Villegas C, Perez R, Sterner O, González-Chavarría I, Paz C. Curcuma as an adjuvant in colorectal cancer treatment. *Life Sci.* 2021;286. doi:10.1016/j.lfs.2021.120043
16. Kongpol K, Sermkaew N, Makkliang F, et al. Extraction of curcuminoids and ar-turmerone from turmeric (*curcuma longa* L.) using hydrophobic deep eutectic solvents (HDESs) and application as HDES-based microemulsions. *Food Chem.* 2022;396:133728. doi:10.1016/J.foodchem.2022.133728
17. Toden S, Theiss AL, Wang X, Goel A. Essential turmeric oils enhance anti-inflammatory efficacy of curcumin in dextran sulfate sodium-induced colitis. *Sci Rep.* 2017;7(1):1–12. doi:10.1038/s41598-017-00812-6
18. Kraist P, Hirun N, Mahadlek J, Limmatvapirat S. Fluconazole-loaded solid lipid nanoparticles (SLNs) as a potential carrier for buccal drug delivery of oral candidiasis treatment using the box-behnken design. *J Drug Deliv Sci Technol.* 2021;63:102437. doi:10.1016/j.jddst.2021.102437
19. Raja HN, Din F U, Shabbir K, et al. Sodium alginate-based smart gastro-retentive drug delivery system of revaprazan loaded SLNs; formulation and characterization. *Int J Biol Macromol.* 2023;253:127402. doi:10.1016/j.ijbiomac.2023.127402
20. Kuchler S, Herrmann W, Panek-Minkin G, et al. SLN for topical application in skin diseases—characterization of drug-carrier and carrier-target interactions. *Int J Pharm.* 2010;390(2):225–233. doi:10.1016/j.ijpharm.2010.02.004
21. Pawar KR, Babu RJ. Polymeric and lipid-based materials for topical nanoparticle delivery systems. *Crit Rev Ther Drug Carr Syst.* 2010;27(5):419–459. doi:10.1615/critrevtherdrugcarriersyst.v27.i5.20
22. Rapalli VK, Sharma S, Roy A, Alexander A, Singhvi G. Solid lipid nanocarriers embedded hydrogel for topical delivery of apremilast: in-vitro, ex-vivo, dermatopharmacokinetic and anti-psoriatic evaluation. *J Drug Deliv Sci Technol.* 2021;63:102442. doi:10.1016/j.jddst.2021.102442
23. Gönüllü Ü, Üner M, Yener G, Karaman EF, Aydoğmuş Z. Formulation and characterization of solid lipid nanoparticles, nanostructured lipid carriers and nanoemulsion of lornoxicam for transdermal delivery. *Acta Pharm.* 2015;65(1):1–13. doi:10.1515/acph-2015-0009
24. Liu M, Sharma M, Lu GL, Zhang Z, Yin N, Wen J. Full factorial design, physicochemical characterization, ex vivo investigation, and biological assessment of glutathione-loaded solid lipid nanoparticles for topical application. *Int J Pharm.* 2023;630:122381. doi:10.1016/j.ijpharm.2022.122381
25. Souto EB, Wissing SA, Barbosa CM, Müller RH. Development of a controlled release formulation based on SLN and NLC for topical clotrimazole delivery. *Int J Pharm.* 2004;278(1):71–77. doi:10.1016/j.ijpharm.2004.02.032
26. Schäfer-Korting M, Mehnert W, Korting HC. Lipid nanoparticles for improved topical application of drugs for skin diseases. *Adv Drug Deliv Rev.* 2007;59(6):427–443. doi:10.1016/j.addr.2007.04.006
27. Pardeike J, Hommoss A, Müller RH. Lipid nanoparticles (SLN, NLC) in cosmetic and pharmaceutical dermal products. *Int J Pharm.* 2009;366(1–2):170–184. doi:10.1016/j.ijpharm.2008.10.003
28. Raina N, Rani R, Thakur VK, Gupta M. New insights in topical drug delivery for skin disorders: from a nanotechnological perspective. *ACS Omega.* 2023;8(22):19145–19167. doi:10.1021/acsomega.2c08016/asset/images/large/ao2c08016
29. Hemrajani C, Negi P, Parashar A, et al. Overcoming drug delivery barriers and challenges in topical therapy of atopic dermatitis: a nanotechnological perspective. *Biomed Pharmacother.* 2022;147:112633. doi:10.1016/j.biopha.2022.112633
30. Jain AK, Jain S, Abourehab MAS, Mehta P, Kesharwani P. An insight on topically applied formulations for management of various skin disorders. *J Biomater Sci Polym Ed.* 2022;33(18):2406–2432. doi:10.1080/09205063.2022.2103625
31. Shah KA, Date AA, Joshi MD, Patravale VB. Solid lipid nanoparticles (SLN) of tretinoin: potential in topical delivery. *Int J Pharm.* 2007;345(1–2):163–171. doi:10.1016/j.ijpharm.2007.05.061
32. Mandawgade SD, Patravale VB. Development of SLNs from natural lipids: application to topical delivery of tretinoin. *Int J Pharm.* 2008;363(1–2):132–138. doi:10.1016/j.ijpharm.2008.06.028
33. Kaur K, Jindal R, Jindal D. RSM-CCD optimized microwave-assisted synthesis of chitosan and gelatin-based pH sensitive, inclusion complexes incorporated hydrogels and their use as controlled drug delivery systems. *J Drug Deliv Sci Technol.* 2018;48:161–173. doi:10.1016/j.jddst.2018.09.003
34. Aksu B, Paradkar A, De Matas M, Özer Ö, Güneri T, York P. A quality by design approach using artificial intelligence techniques to control the critical quality attributes of ramipril tablets manufactured by wet granulation. *Pharm Dev Technol.* 2013;18(1):236–245. doi:10.3109/10837450.2012.705294
35. Gonzalez-Mira E, Egea MA, Souto EB, Calpena AC, Garcia ML. Optimizing flurbiprofen-loaded NLC by central composite factorial design for ocular delivery. *Nanotechnology.* 2011;22(4). doi:10.1088/0957-4484/22/4/045101
36. Varshosaz J, Ghaffari S, Khoshayand MR, Atyabi F, Azarmi S, Kobarfard F. Development and optimization of solid lipid nanoparticles of amikacin by central composite design. *J Liposome Res.* 2010;20(2):97–104. doi:10.3109/08982100903103904

37. Alhakamy NA, Hosny KM, Aldryhim AY, et al. Development and optimization of ofloxacin as solid lipid nanoparticles for enhancement of its ocular activity. *J Drug Deliv Sci Technol.* 2022;72:103373. doi:10.1016/j.jddst.2022.103373
38. Behbahani ES, Ghaedi M, Abbaspour M, Rostamizadeh K. Optimization and characterization of ultrasound assisted preparation of curcumin-loaded solid lipid nanoparticles: application of central composite design, thermal analysis and X-ray diffraction techniques. *Ultrason Sonochem.* 2017;38:271–280. doi:10.1016/j.ultsonch.2017.03.013
39. Dourado D, Oliveira MC D, Araujo GRS D, et al. Low-surfactant microemulsion, a smart strategy intended for curcumin oral delivery. *Colloids Surf a Physicochem Eng Aspects.* 2022;652:129720. doi:10.1016/j.colsurfa.2022.129720
40. Schubert MA, Müller-Goymann CC. Characterisation of surface-modified solid lipid nanoparticles (SLN): influence of lecithin and nonionic emulsifier. *Eur J Pharm Biopharm.* 2005;61(1–2):77–86. doi:10.1016/j.ejpb.2005.03.006
41. Shrotriya S, Ranpise N, Satpute P, Vidhate B. Skin targeting of curcumin solid lipid nanoparticles-engrossed topical gel for the treatment of pigmentation and irritant contact dermatitis. *Cells Nanomed Biotechnol.* 2018;46(7):1471–1482. doi:10.1080/21691401.2017.1373659
42. Hassan H, Adam SK, Alias E, Affandi MRRMM, Shamsuddin AF, Basir R. Central composite design for formulation and optimization of solid lipid nanoparticles to enhance oral bioavailability of Acyclovir. *Molecules.* 2021;26(18). doi:10.3390/molecules26185432
43. Sağıroğlu AA, Özsoy Y, Özer Ö. Design, optimization and characterization of novel topical formulations containing Triamcinolone Acetonide. *J Drug Deliv Sci Technol.* 2020;58:101594. doi:10.1016/j.jddst.2020.101594
44. Chao IC, Wang CM, Li SP, Lin LG, Ye WC, Zhang QW. Simultaneous quantification of three curcuminoids and three volatile components of curcuma longa using pressurized liquid extraction and high-performance liquid chromatography. *Mol.* 2018;23:Page 1568. doi:10.3390/molecules23071568
45. Lin X, Li X, Zheng LQ, Yu L, Zhang Q, Liu W. Preparation and characterization of monocaprates nanostructured lipid carriers. *Colloids Surf a Physicochem Eng Aspects.* 2007;311(1–3):106–111. doi:10.1016/j.colsurfa.2007.06.003
46. Singh S, Kushwaha AK, Vuddanda PR, Karunanidhi P, Singh SK. Development and evaluation of solid lipid nanoparticles of raloxifene hydrochloride for enhanced bioavailability. *Biomed Res Int.* 2013;2013:1. doi:10.1155/2013/584549
47. Jourghanian P, Ghaffari S, Ardjmand M, Haghighat S, Mohammadnejad M. Sustained release curcumin loaded solid lipid nanoparticles. *Adv Pharm Bull.* 2016;6(1):17. doi:10.15171/apb.2016.04
48. Freitas C, Müller RH. Effect of light and temperature on zeta potential and physical stability in solid lipid nanoparticle (SLN<sup>TM</sup>) dispersions. *Int J Pharm.* 1998;168(2):221–229. doi:10.1016/S0378-5173(98)00092-1
49. Amelian A, Wasilewska K, Megias D, Winnicka K. Application of standard cell cultures and 3D in vitro tissue models as an effective tool in drug design and development. *Pharmacol Rep.* 2017;69(5):861–870. doi:10.1016/j.pharep.2017.03.014
50. Kidd DA, Johnson M, Clements J. Development of an in vitro corrosion/irritation prediction assay using the EpiDerm<sup>TM</sup> skin model. *Toxicol Vitr.* 2007;21(7):1292–1297. doi:10.1016/J.TIV.2007.08.018
51. Kandárová H, Hayden P, Klausner M, Kubilus J, Sheasgreen J. An in vitro skin irritation Test (SIT) using the epiderm reconstructed human epidermal (RHE) model. *JoVE (Journal Vis Exp).* 2009;(29):e1366. doi:10.3791/1366
52. Li L, Mou X, Xie H, et al. In vitro tests to evaluate embryotoxicity and irritation of Chinese herbal medicine (pentaherbs formulation) for atopic dermatitis. *J Ethnopharmacol.* 2023;305:116149. doi:10.1016/j.jep.2023.116149
53. Nair R, Kumar AC, Priya VK, Yadav CM, Raju PY. Formulation and evaluation of chitosan solid lipid nanoparticles of carbamazepine. *Lipids Health Dis.* 2012;11(1):1–8. doi:10.1186/1476-511X-11-72/tables/5
54. Musielak E, Feliczak-Guzik A, Nowak I. Optimization of the conditions of solid lipid nanoparticles (SLN) synthesis. *Molecules.* 2022;27(7). doi:10.3390/molecules27072202
55. Rahmanian-Devin P, Askari VR, Sanei-Far Z, et al. Preparation and characterization of solid lipid nanoparticles encapsulated nospapine and evaluation of its protective effects against imiquimod-induced psoriasis-like skin lesions. *Biomed Pharmacother.* 2023;168:115823. doi:10.1016/j.biopha.2023.115823
56. Emami J, Mohiti H, Hamishehkar H, Varshosaz J. Formulation and optimization of solid lipid nanoparticle formulation for pulmonary delivery of budesonide using Taguchi and box-behnken design. *Res Pharm Sci.* 2015;10(1):17.
57. Ekambaram P, Abdul Hasan Sathali A. Formulation and evaluation of solid lipid nanoparticles of ramipril. *J Young Pharm.* 2011;3(3):216. doi:10.4103/0975-1483.83765
58. Kovacevic A, Savic S, Vuleta G, Müller RH, Keck CM. Polyhydroxy surfactants for the formulation of lipid nanoparticles (SLN and NLC): effects on size, physical stability and particle matrix structure. *Int J Pharm.* 2011;406(1–2):163–172. doi:10.1016/j.ijpharm.2010.12.036
59. Kovačević AB, Müller RH, Savić SD, Vuleta GM, Keck CM. Solid lipid nanoparticles (SLN) stabilized with polyhydroxy surfactants: preparation, characterization and physical stability investigation. *Colloids Surf a Physicochem Eng Aspects.* 2014;444:15–25. doi:10.1016/j.colsurfa.2013.12.023
60. Xing R, Mustapha O, Ali T, et al. Development, characterization, and evaluation of sln-loaded thermoresponsive hydrogel system of Topotecan as biological macromolecule for colorectal delivery. *Biomed Res Int.* 2021. doi:10.1155/2021/9968602
61. Mukherjee S, Ray S, Thakur RS. Solid lipid nanoparticles: a modern formulation approach in drug delivery system. *Indian J Pharm Sci.* 2009;71(4):349. doi:10.4103/0250-474x.57282
62. Levy MY, Schutze W, Fuhrer C, Benita S. Characterization of diazepam submicron emulsion interface: role of oleic acid. *J Microencapsul.* 1994;11(1):79–92. doi:10.3109/02652049409040440
63. Souto EB, Wissing SA, Barbosa CM, Müller RH. Evaluation of the physical stability of SLN and NLC before and after incorporation into hydrogel formulations. *Eur J Pharm Biopharm.* 2004;58(1):83–90. doi:10.1016/j.ejpb.2004.02.015
64. Uner B, Ozdemir S, Yildirim E, et al. Loteprednol loaded nanoformulations for corneal delivery: ex-vivo permeation study, ocular safety assessment and stability studies. *J Drug Deliv Sci Technol.* 2023;81:104252. doi:10.1016/j.jddst.2023.104252
65. Stahl MA, Lüdtkke FL, Grimaldi R, Gigante ML, Ribeiro APB. Characterization and stability of solid lipid nanoparticles produced from different fully hydrogenated oils. *Food Res Int.* 2024;176:113821. doi:10.1016/j.foodres.2023.113821
66. Pinzaru I, Tanase A, Enatescu V, et al. Proniosomal gel for topical delivery of rutin: preparation, physicochemical characterization and in vitro toxicological profile using 3d reconstructed human epidermis tissue and 2d cells. *Antioxidants.* 2021;10(1):1–21. doi:10.3390/antiox10010085
67. Hayden PJ, Bachelor M, Ayeahunie S, et al. Application of mattek in vitro reconstructed human skin models for safety, efficacy screening, and basic preclinical research. *Applied in vitro Toxicology.* 2015;1(3):226–233. doi:10.1089/aivt.2015.0012
68. Vinardell MP, Mitjans M. Alternative methods for eye and skin irritation tests: an overview. *J Pharm Sci.* 2008;97(1):46–59. doi:10.1002/jps.21088

69. Test N. 439: in vitro skin irritation: reconstructed human epidermis test method. *OECD Guidel Test Chem Sec.* 2021;4:1. doi:10.1787/9789264242845-en.
70. Kidd DA, Johnson M, Clements J. Development of an in vitro corrosion/irritation prediction assay using the epiderm skin model. *Toxicol In Vitro.* 2007;21(7):1292–1297. doi:10.1016/j.tiv.2007.08.018
71. Harde H, Agrawal AK, Katariya M, Kale D, Jain S. Development of a topical adapalene-solid lipid nanoparticle loaded gel with enhanced efficacy and improved skin tolerability. *RSC Adv.* 2015;5(55):43917–43929. doi:10.1039/c5ra06047h

International Journal of Nanomedicine

Dovepress

## Publish your work in this journal

The International Journal of Nanomedicine is an international, peer-reviewed journal focusing on the application of nanotechnology in diagnostics, therapeutics, and drug delivery systems throughout the biomedical field. This journal is indexed on PubMed Central, MedLine, CAS, SciSearch®, Current Contents®/Clinical Medicine, Journal Citation Reports/Science Edition, EMBase, Scopus and the Elsevier Bibliographic databases. The manuscript management system is completely online and includes a very quick and fair peer-review system, which is all easy to use. Visit <http://www.dovepress.com/testimonials.php> to read real quotes from published authors.

Submit your manuscript here: <https://www.dovepress.com/international-journal-of-nanomedicine-journal>